

# Synthesis of Graphdiyne Nanowalls Using Acetylenic Coupling Reaction

Jingyuan Zhou,<sup>†,‡</sup> Xin Gao,<sup>†</sup> Rong Liu,<sup>†,‡</sup> Ziqian Xie,<sup>†</sup> Jin Yang,<sup>‡,§</sup> Shuqing Zhang,<sup>†,‡</sup> Gengmin Zhang,<sup>§</sup> Huibiao Liu,<sup>||</sup> Yuliang Li,<sup>||</sup> Jin Zhang,<sup>\*,†</sup> and Zhongfan Liu<sup>\*,†</sup>

<sup>†</sup>Center for Nanochemistry, Beijing Science and Engineering Center for Nanocarbons, Beijing National Laboratory for Molecular Sciences, College of Chemistry and Molecular Engineering, <sup>‡</sup>Academy for Advanced Interdisciplinary Studies, and <sup>§</sup>Key Laboratory for the Physics and Chemistry of Nanodevices and Department of Electronics, Peking University, Beijing 100871, PR China

<sup>||</sup>Institute of Chemistry, Chinese Academy of Sciences, Beijing 100190, PR China

## Supporting Information

**ABSTRACT:** Synthesizing graphdiyne with a well-defined structure is a great challenge. We reported herein a rational approach to synthesize graphdiyne nanowalls using a modified Glaser–Hay coupling reaction. Hexaethynylbenzene and copper plate were selected as monomer and substrate, respectively. By adjusting the ratio of added organic alkali along with the amount of monomer, the proper amount of copper ions was dissolved into the solution, thus forming catalytic reaction sites. With a rapid reaction rate of Glaser–Hay coupling, graphdiyne grew vertically at these sites first, and then with more copper ions dissolved, uniform graphdiyne nanowalls formed on the surface of copper substrate. Raman spectra, UV–vis spectra, and HRTEM results confirmed the features of graphdiyne. These graphdiyne nanowalls also exhibited excellent and stable field-emission properties.

Over the past two decades, tremendous efforts have been devoted to searching new carbon allotropes where novel forms such as fullerene,<sup>1</sup> carbon nanotubes,<sup>2</sup> and graphene<sup>3</sup> have been added to the family. All-carbon materials possessing certain advantages of light weight, flexibility and diverse fabrication approaches have been studied experimentally and theoretically.<sup>4</sup> Different types of carbon allotropes have been constituted by altering the periodic binding motif in networks consisted of sp, sp<sup>2</sup>, and sp<sup>3</sup> hybridized carbon atoms.<sup>5</sup> Specifically, graphyne, which was first proposed by Baughman in 1987,<sup>6</sup> refers to a family of carbon allotropes merely composed of sp- and sp<sup>2</sup>-hybridized carbon atoms extending in a 2D plane. Among various predicted structures, graphdiyne is a certain framework containing hexagonal benzene rings connected by diacetylenic linkages. It is predicted to be the most stable carbon network containing diacetylenic linkages with a heat of formation of 18.3 kcal per gram of atoms C.<sup>7</sup> With a highly conjugated structure, remarkable electronic properties,<sup>8</sup> uniformly distributed pores, and distinct optical properties, graphdiyne is forecasted to be promising for various applications in semiconductor devices,<sup>9</sup> electrode material,<sup>10</sup> lithium storage,<sup>11</sup> hydrogen storage,<sup>12</sup> gas separation,<sup>13</sup> high third-order nonlinear optical (NLO) susceptibility material,<sup>14</sup> solar cells,<sup>15</sup> etc. Meanwhile, it also exhibits great photocatalytic performance when hybridized with TiO<sub>2</sub> or Ag/AgBr.<sup>16,17</sup>

To date, several attempts have been reported about establishing feasible pathways for the preparation of graphdiyne. Pioneer work was concerned with employing convergent synthesis to synthesize a series of building blocks of graphdiyne based on dehydrobenzoannulenes.<sup>18,19</sup> Attempts to graphdiyne preparation were also conducted in UHV system where some six-membered oligomeric cyclic units were synthesized with the assistance of metal surface.<sup>20</sup> However, such routes mentioned above are not applicable to scalable synthesis of graphdiyne. In 2010, a graphdiyne film with a thickness of nearly 1 μm was successfully fabricated on the surface of copper foil via an in situ Glaser coupling reaction.<sup>21</sup> Since then, several follow-up studies reported the achievement of various morphologies of graphdiyne, e.g., graphdiyne nanotubes<sup>22</sup> and graphdiyne nanowires<sup>23</sup> through a template-assisted method and a vapor-transport process, respectively. However, explicit component characterization and morphology-controlled synthesis of graphdiyne are still in their infancy. Achieving graphdiyne with different well-defined structures and distinct properties may make a significant contribution to both basic study and development process of such a new type of carbon allotrope.

Herein, we report a feasible synthesis route of graphdiyne nanowalls by employing a modified Glaser–Hay coupling. Glaser coupling is a classic reaction to prepare 1,3-diyne,<sup>24</sup> and it has also been proven beneficial to the synthesis of graphdiyne film.<sup>21</sup> For the structural control of nanomaterials, catalyst distribution and monomer concentration are critical factors.<sup>26</sup> It would appear that Glaser–Hay coupling is a good candidate for synthesizing graphdiyne with a well-defined structure. It is a crucial modification reported by Hay indicating that addition of catalytic amount of a nitrogen ligand *N,N,N',N'*-tetramethylethylenediamine (TMEDA) allowed the coupling reaction to be carried out with a rapid rate in other nonalkaline solutions such as acetone.<sup>25</sup> There are several merits of this reaction. First, the coupling yield can be promoted because of the enhanced solubility of the reactive species. Second, the generation of copper ions can be properly tuned by additional amounts of alkali so that the reaction sites could be regulated. Finally, with a faintly acidic property of terminal alkyne, the monomer hexaethynylbenzene (HEB) is supposed to be more stable in

Received: April 20, 2015

Published: June 5, 2015

acetone solution rather than in pyridine with weak acidity. By adjusting the ratio of pyridine and TMEDA and the concentration of monomer, graphdiyne nanowalls were observed, and after that, the morphology, composition, and structure of graphdiyne nanowalls were studied systematically. Notably, the unique structures with the conjugated plane and abundant vertical sharp sheets enable graphdiyne nanowalls to exhibit excellent and stable field-emission performance.

The schematic illustration of the synthesis process is depicted in Figure 1a. Graphdiyne nanowalls were prepared through a

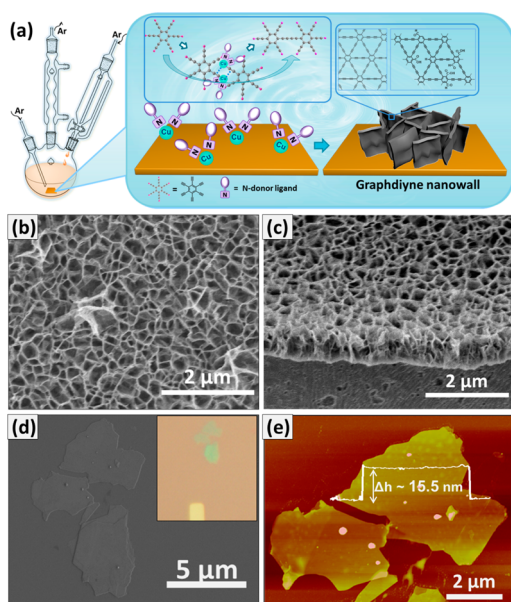


**Figure 1.** (a) Schematic illustration of the experimental setup. SEM images of graphdiyne nanowalls on Cu substrate: (b) top view, (c) cross-sectional view. (d) SEM image and OM image (inset) of an exfoliated sample. (e) AFM image of an exfoliated sample on Si/SiO<sub>2</sub> substrate. The height profile is taken along the white line, representing a 15.5 nm thick film.

modified Glaser–Hay coupling reaction with HEB as precursor. The commonly employed copper salt catalyst was replaced by Cu plates. Briefly, copper plates were placed in the mixed solution of acetone, pyridine, and TMEDA with proper ratio; then, an acetone solution of procedure was added in a dropwise manner. (See Supporting Information for details.) Copper is easy to convert to Cu ions in the presence of a catalytic amount of base,<sup>21</sup> where a Glaser–Hay reaction took place efficiently with the aid of TMEDA. By adjusting the dosage of N ligands, graphdiyne nanowalls could be uniformly grown on Cu plates.

The morphology of the as-prepared graphdiyne nanowalls was characterized by scanning electron microscopy (SEM). Figure 1b,c shows typical SEM images, top and cross-sectional views, respectively. Surprisingly, it was found that continuous matrix of vertically erected nanowalls possessed large voids submicrometers in diameter. The cross-sectional view suggests these vertical walls are around hundreds of nanometers high. Actually, the distribution of the nanowalls is remarkably uniform over the whole substrate surface (typically 1 × 2 cm<sup>2</sup>). Furthermore, SEM and atomic force microscopy (AFM) characterization (Figure 1d,e) of mechanically exfoliated sample transferred on Si/SiO<sub>2</sub> substrate indicate that such walls are of layered structures with thicknesses ranging from several to dozens of nanometers.

Figure 2a displays a transmission electron microscopy (TEM) observation of as-obtained graphdiyne nanowalls,

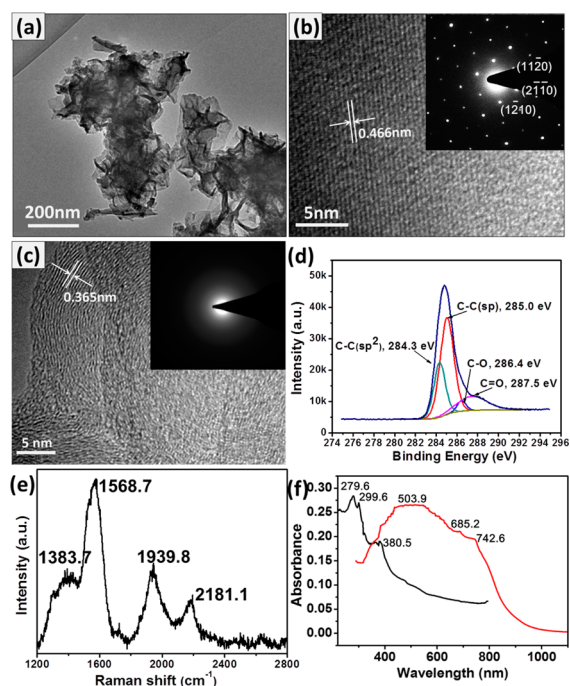


**Figure 2.** (a) TEM image and (b and c) HRTEM images of graphdiyne nanowalls; related SAED patterns are in corresponding insets. (d) XPS spectra of graphdiyne nanowalls for C 1s. (e) Raman spectra and (f) UV–vis spectra of graphdiyne nanowalls.

verifying that the walls are flat and continuous. High-resolution TEM (HRTEM) characterization and corresponding selected-area electron diffraction (SAED) patterns reveal the high crystallinity of graphdiyne nanowalls in certain areas (Figure 2b). The lattice fringe is 0.466 nm in good agreement with the theoretical result.<sup>8</sup> Additionally, another form of crystal lattice is shown in Figure 2c. It clearly reveals curved streaks with a lattice parameter of 0.365 nm, which can be assigned to the spacing between carbon layers,<sup>9,27</sup> suggesting the presence of curved graphdiyne sheets. This value is a slightly higher than that of graphene<sup>28</sup> owing to a more delocalized system of graphdiyne. Moreover, the interlayer spacing value was also studied theoretically. With different stacking configurations, the value varies within the range of 0.340–0.365 nm.<sup>29</sup>

In addition, the elementary composition and bonding structure were studied systematically with X-ray photoelectron spectroscopy (XPS), Raman spectroscopy, and UV–vis absorption spectroscopy separately. The spectra of XPS indicate that the graphdiyne nanowalls are mainly composed of elemental carbon (Figure S4), which is identical to the result of energy-dispersive spectrometry (EDS) in Figure S5. The peak at 284.8 eV shows essentially identical binding energy for the C 1s orbital. In detail, the peak of C 1s can be deconvoluted into four subpeaks, corresponding to sp<sup>2</sup> (benzene rings) at binding energy of 284.5 eV, sp (C≡C) at 285.2 eV, C–O at 286.4 eV, and C=O at 287.5 eV, respectively.<sup>30</sup> The presence of elemental O derives from the adsorption of air in the pores of nanowalls and small amounts of oxygen-containing of groups. They come from oxidation of some terminal alkyne, resulting in some defects. Beyond that, Raman spectroscopy is a powerful tool to monitor Raman-active carbon–carbon triple

bonds. As shown in Figure 2e, the Raman spectrum displays four prominent peaks around 1383.7, 1568.7, 1939.8, and 2181.1  $\text{cm}^{-1}$ , which are consistent with previously reported values.<sup>21</sup> The peak at 1383.7  $\text{cm}^{-1}$  corresponds to the breathing vibration of  $\text{sp}^2$  carbon domains in aromatic rings (D band). The peak at 1568.7  $\text{cm}^{-1}$  is due to the first-order scattering of the  $\text{E}_{2g}$  mode for in-phase stretching vibration of  $\text{sp}^2$  carbon lattice in aromatic rings (G band).<sup>30</sup> The peak at 2181.1  $\text{cm}^{-1}$  can be attributed to the vibration of conjugated diyne links.<sup>21</sup> As for terminal alkyne monomers, a sharp peak around 2106  $\text{cm}^{-1}$  can be detected for carbon–carbon triple bond stretching (Figure S6). When it reacts to diyne linkage, there will be an obvious hypochromatic shift to 2181.1  $\text{cm}^{-1}$ . However, we have not found explicit theoretical assignment to 1939.8  $\text{cm}^{-1}$ . Careful analysis of our experimental system indicates that it can only be assigned to some vibration related to carbon–carbon triple bonds, and previous work expressed the same view.<sup>21</sup> Relevant theoretical research has also been reported by our group and revealed similar results.<sup>31</sup> To investigate the optical properties of as-prepared graphdiyne nanowalls, UV–vis absorption analysis was also employed. Some previous studies have demonstrated the correlation between the number of chromophores and the absorbance frequency. Compared with the monomer, there is an obvious bathochromic shift in the UV–vis spectra (Figure 2f), indicating enhanced electron delocalization through the extendedly conjugated  $\pi$  system.<sup>32</sup>

Concerning the growing mechanism of graphdiyne nanowalls, we tried to trace the process of the reaction, and a feasible mechanism of the process can be proposed and divided into three steps (as shown in Figure 3a). First, with the presence of

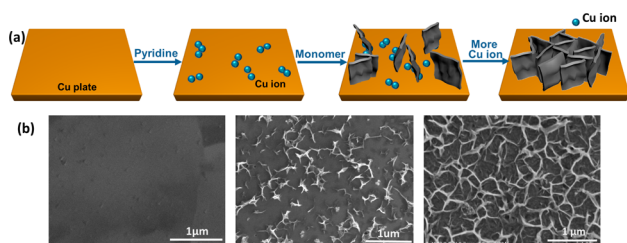


**Figure 3.** (a) Proposed reaction process of graphdiyne nanowalls. (b) SEM images of the formation process of graphdiyne nanowalls in time series (from left to right, respectively): bare Cu plate before reaction and 8 and 10 h after reaction.

a pyridine molecule, a small amount copper ions generated on the surface of copper plates and dissolved into the solution act as catalyst in the initial stage of reaction. Second, at these catalytically active sites, the Glaser–Hay coupling reaction occurred immediately with the presence of TMEDA. Because the concentration of monomer solution was very low and it was introduced by dripping slowly, only small amount of monomers reacted at these sites, forming some single vertical graphdiyne nanosheets. Finally, as the reaction progressed, more Cu ion dissolved into the solution, and graphdiyne nanowalls became more compact. Figure 4b shows the process as described above corresponding to sequential time series. If more pyridine was added, then more random structures could be observed (shown in Figure S7) because too many copper ions came into the solution in a short time, so the formation of graphdiyne nanowalls originated from two factors: the slow release of catalyst concentration and the rapid reaction rate of this reaction.

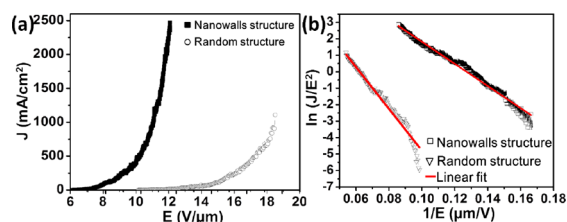


**Figure 4.** (a) Typical plots of the electron-emission current density ( $J$ ) as a function of applied electric field ( $E$ ). (b) Corresponding F–N plots and linear fitting.

For further explanation, the Cu plate was exposed to air after pretreatment so that a small amount of metallic oxide formed on the surface. As shown in Figure S7, the oxidation state of copper can be observed from the XPS spectra. Thus, we consider that the valence ascending of copper is ascribed to the oxidation, and copper ions in reaction solution were also detected by inductively coupled plasma (ICP) analysis (Table S1). It has been confirmed that Cu(II) could be reduced by phenylacetylene to Cu(I). The homocoupling procedure completes via a Cu(I)–Cu(II) synergistic reaction, and Cu(I) plays a role as catalyst.<sup>33</sup> From this point of view, both species of Cu ion can form catalytically active centers.

With a highly conjugated structure and uniformly distributed sharp walls, graphdiyne nanowalls are believed to exhibit superior field-emission performance. The field-emission properties of as-prepared graphdiyne nanowalls are in Figure 4. Figure 4a shows the typical plot of emission current density  $J$  versus the applied electric field ( $J$ – $E$  curve). The  $E_{\text{to}}$  (turn-on field) is about 6.6  $\text{V}/\mu\text{m}$ , and  $E_{\text{thr}}$  (threshold field) is 10.7  $\text{V}/\mu\text{m}$ . Figure 4b shows the corresponding Fowler–Nordheim (F–N) plots and the corresponding fitted curve. The curve is very consistent with the F–N mechanism, indicating that the electron emission from the samples is a result of electron tunneling.<sup>34</sup> The value of  $E_{\text{to}}$  is higher than that of vertical graphene nanosheets<sup>35</sup> because the carrier mobility of graphdiyne is much lower than that of graphene.<sup>8</sup> However, the value of  $E_{\text{to}}$  is still considerably low among commonly used field-emission devices. In all, graphdiyne nanowalls exhibit good field-emission properties consistent with F–N theory. From the SEM images of comparison between the nanowalls morphology before and after field-emission test (Figure S8), it can be seen that some walls were destroyed under a high current, whereas others were intact. Furthermore, in contrast, the field-emission properties of graphdiyne with random mentioned above showed substantially higher  $E_{\text{to}}$  (12.6  $\text{V}/\mu\text{m}$ ) and  $E_{\text{thr}}$  (16.3  $\text{V}/\mu\text{m}$ ) because of the lack of emission tips. The results show the following conclusions. First, the graphdiyne nanowalls are consistently of high density of effective emission tips, e.g., the edges of vertically oriented thin walls as shown in Figure 1. Second, some regions of the sample were merely with amorphization or lower polymerization degree that could not endure a strong current and were burned. Finally, the sheets of graphdiyne nanowalls with regular structure are tolerant to a high current attributed to the conjugated structure, indicating graphdiyne as a candidate for all-carbon electric devices.

For the first time, graphdiyne nanowalls were synthesized successfully via a modified Glaser–Hay coupling reaction by regulating the catalytically active sites. It bears typical Raman peaks of diyne and benzene rings along with lattice spacing of 0.466 nm. Also, such novel morphology of graphdiyne has shown extraordinary and stable field-emission properties. The



strategy used here has thrown a glimmer of light on the exploration of graphdiyne construction with a well-defined nanostructure. With a better understanding of the reaction process, it is promising to synthesize large domains of graphdiyne with high crystallization and study some basic properties of graphdiyne.

## ■ ASSOCIATED CONTENT

### ■ Supporting Information

Experimental details, characterization methods, and supplementary figures. The Supporting Information is available free of charge on the ACS Publications website at DOI: 10.1021/jacs.5b04057.

## ■ AUTHOR INFORMATION

### Corresponding Authors

\*jinzhang@pku.edu.cn

\*zfliu@pku.edu.cn

### Notes

The authors declare no competing financial interest.

## ■ ACKNOWLEDGMENTS

We thank Jinying Wang and Zhenzhu Li for valuable discussion from the perspective of theoretical calculation. This work was financially supported by the Ministry of Science and Technology of China (grants 2013CB932603 and 2012CB933404), the National Natural Science Foundation of China (grant 51432002), and the Ministry of Education (20120001130010).

## ■ REFERENCES

- (1) Kroto, H. W.; Allaf, A. W.; Balm, S. P. *Chem. Rev.* **1991**, *91*, 1213.
- (2) Iijima, S. *Nature* **1991**, *354*, 56.
- (3) Novoselov, K. S.; Geim, A. K.; Morozov, S. V.; Jiang, D.; Zhang, Y.; Dubonos, S. V.; Grigorieva, I. V.; Firsov, A. A. *Science* **2004**, *306*, 666.
- (4) Diederich, F. *Nature* **1994**, *369*, 199.
- (5) Heimann, R. B.; Koga, Y. *Carbon* **1997**, *35*, 1654.
- (6) Baughman, R. H.; Eckhardt, H.; Kertesz, M. *J. Chem. Phys.* **1987**, *87*, 6687.
- (7) Wan, W. B.; Brand, S. C.; Pak, J. J.; Haley, M. M. *Chem.—Eur. J.* **2000**, *6*, 2044.
- (8) Long, M. Q.; Tang, L.; Wang, D.; Li, Y. L.; Shuai, Z. G. *ACS Nano* **2011**, *5*, 2593.
- (9) Qian, X. M.; Liu, H. B.; Huang, C. S.; Chen, S. H.; Zhang, L.; Li, Y. J.; Wang, J. Z.; Li, Y. L. *Sci. Rep.* **2015**, *5*, 7756.
- (10) (a) Sun, C.; Searles, D. J. *J. Phys. Chem. C* **2012**, *116*, 26222. (b) Zhang, H.; Xia, Y.; Bu, H.; Wang, X.; Zhang, M.; Luo, Y.; Zhao, M. *J. Appl. Phys.* **2013**, *113*, 044309.
- (11) Huang, C. S.; Zhang, S. L.; Liu, H. B.; Li, Y. J.; Cui, G. L.; Li, Y. L. *Nano Energy* **2015**, *11*, 481.
- (12) Hwang, H. J.; Lee, H. J. *J. Phys. Chem. C* **2012**, *116*, 20220.
- (13) Cranford, S. W.; Buehler, M. J. *Nanoscale* **2012**, *4*, 4587.
- (14) Bhaskar, A.; Guda, R.; Haley, M. M.; Goodson, J. *Am. Chem. Soc.* **2006**, *128*, 13972.
- (15) Xiao, J.; Shi, J.; Liu, H.; Xu, Y.; Lv, S.; Luo, Y.; Li, D.; Meng, Q.; Li, Y. *Adv. Energy Mater.* **2015**, *5*, 1401943.
- (16) Yang, N. L.; Liu, Y. Y.; Wen, H.; Tang, Z. Y.; Zhao, H. J.; Li, Y. L.; Wang, D. *ACS Nano* **2013**, *7*, 1504.
- (17) Zhang, X.; Zhu, M. S.; Chen, P. L.; Li, Y. J.; Liu, H. B.; Li, Y. L.; Liu, M. H. *J. Phys. Chem. Chem. Phys.* **2015**, *17*, 1217.
- (18) Haley, M. M.; Brand, S. C.; Pak, J. J. *Angew. Chem., Int. Ed. Engl.* **1997**, *36*, 836.
- (19) Johnson, C. A.; Lu, Y.; Haley, M. M. *Org. Lett.* **2007**, *9*, 3725.

- (20) Zhang, Y. Q.; Kepčija, N.; Kleinschrodt, M.; Diller, K.; Fischer, S.; Papageorgiou, A. C.; Allegretti, F.; Björk, J.; Klyatskaya, S.; Klappenberger, F.; Ruben, M.; Barth, J. V. *Nat. Commun.* **2012**, *3*, 1286.
- (21) Li, G. X.; Li, Y. L.; Liu, H. B.; Guo, Y. B.; Li, Y. J.; Zhu, D. B. *Chem. Commun.* **2010**, *46*, 3256.
- (22) Li, G. X.; Li, Y. L.; Qian, X. M.; Liu, H. B.; Lin, H. W.; Chen, N.; Li, Y. J. *J. Phys. Chem. C* **2011**, *115*, 2611.
- (23) Qian, X. M.; Ning, Z. Y.; Li, Y. L.; Liu, H. B.; Ouyang, C. B.; Chen, Q.; Li, Y. J. *Dalton Trans.* **2012**, *41*, 730.
- (24) Glaser, C. *Ber. Dtsch. Chem. Ges.* **1869**, *2*, 422.
- (25) Hay, A. S. *J. Org. Chem.* **1962**, *27*, 3320.
- (26) Kumar, B.; Lee, K. Y.; Park, H.-K.; Chae, S. J.; Lee, Y. H.; Kim, S.-W. *ACS Nano* **2011**, *5*, 4197.
- (27) Alexandrou, I. *Phys. Rev. B* **1999**, *60*, 10903.
- (28) Reina, A.; Jia, X.; Ho, J.; Nezich, D.; Son, H.; Bulovic, V.; Dresselhaus, M. S.; Kong, J. *Nano Lett.* **2009**, *9*, 30.
- (29) Zheng, Q.; Luo, G.; Liu, Q.; Quhe, R.; Zheng, J.; Tang, K.; Gao, Z.; Nagase, S.; Lu, J. *Nanoscale* **2012**, *4*, 3990.
- (30) Ferrari, A. C.; Meyer, J. C.; Scardaci, V.; Casiraghi, C.; Lazzeri, M.; Mauri, F.; Piscanec, S.; Jiang, D.; Novoselov, K. S.; Roth, S.; Geim, A. K. *Phys. Rev. Lett.* **2006**, *97*, 187401.
- (31) Wang, J. Y.; Zhang, S. Q.; Zhou, J. Y.; Liu, R.; Du, R.; Xu, H.; Liu, Z. R.; Zhang, J.; Liu, Z. F. *J. Phys. Chem. Chem. Phys.* **2014**, *16*, 11303.
- (32) Luo, G.; Qian, X.; Liu, H.; Qin, R.; Zhou, J.; Li, L.; Gao, Z.; Wang, En.; Mei, W.; Li, Y.; Nagase, S. *Phys. Rev. B* **2011**, *84*, 075439.
- (33) (a) Zhang, G. H.; Yi, H.; Zhang, G.; Deng, Y.; Bai, R. P.; Zhang, H.; Miller, J. T.; Kropf, A. J.; Bunel, E. E.; Lei, An W. *J. Am. Chem. Soc.* **2014**, *136*, 924. (b) Bai, R. P.; Zhang, G. H.; Yi, H.; Huang, Z. L.; Qi, X. T.; Liu, C.; Miller, J. T.; Kropf, A. J.; Bunel, E. E.; Lan, Y.; Lei, An W. *J. Am. Chem. Soc.* **2014**, *136*, 16760.
- (34) Yu, T.; Zhu, Y.; Xu, X.; Shen, Z.; Chen, P.; Lim, C.; Thong, J.; Sow, C. H. *Adv. Mater.* **2005**, *17*, 1595.
- (35) Wu, Z. S.; Pei, S. F.; Ren, W. C.; Tang, D. M.; Gao, L. B.; Liu, B. L.; Li, F.; Liu, C.; Cheng, H. M. *Adv. Mater.* **2009**, *21*, 17.